

NP-LoRA: Null Space Projection Unifies Subject and Style in LoRA Fusion

Chuheng Chen, Xiaofei Zhou, Geyuan Zhang, and Yong Huang

Abstract—Low-Rank Adaptation (LoRA) fusion enables the composition of learned subject and style representations for controllable generation without retraining. However, existing methods rely on weight-based merging within a shared adaptation space, where independently trained LoRAs interfere and degrade fidelity. We show that this interference is fundamentally geometric: content and style LoRAs occupy overlapping, non-orthogonal low-rank subspaces, making weight-based fusion inherently flawed. Analyzing LoRA internal structure, we find that generative behavior is dominated by a few principal directions that must be preserved during fusion. Based on this insight, we reformulate LoRA fusion as a null-space projection problem and propose Null Space Projection LoRA (NP-LoRA), a projection-based framework that enforces subspace separation by construction. NP-LoRA extracts principal style directions via singular value decomposition (SVD) and projects the subject LoRA into the orthogonal complement of the style subspace, preventing interference. We further introduce a soft projection mechanism that provides continuous control over the trade-off between subject fidelity and style preservation. Experiments show that NP-LoRA consistently outperforms strong baselines and generalizes well across pretrained LoRA pairs without retraining.

I. INTRODUCTION

Low-Rank Adaptation (LoRA) [1] has emerged as an efficient customization method for diffusion models [2], [3], [4], [5]. By applying lightweight factorization to attention weights, LoRA learns subject or style-specific representations from a few examples [6]. For flexible reuse of pretrained knowledge in LoRA, a key challenge arises in personalized concept composition: how to combine independently trained content and style LoRAs, which respectively capture subject identity and artistic appearance [7], [8], [9]. Such scenarios commonly arise when users want to render a personalized subject in a desired artistic style, each learned from separate examples. For instance, one may aim to render a learned subject (e.g., a pet dog) in a separately trained artistic style (e.g., Van Gogh’s brushwork), as shown in Fig. 1(a). The goal is to fuse the content LoRA (ΔW_c) and the style LoRA (ΔW_s) into a single coherent module that retains both representations without destructive interference.

Existing merging techniques primarily rely on weight-based operations, which form a weighted combination of LoRAs in parameter space. Recent state-of-the-art approaches, such as ZipLoRA [7], K-LoRA [8], and LoRA.rar [9], move beyond naive linear weight yet still adhere to the paradigm of weight-based fusion. Specifically, ZipLoRA [7] learns an optimal

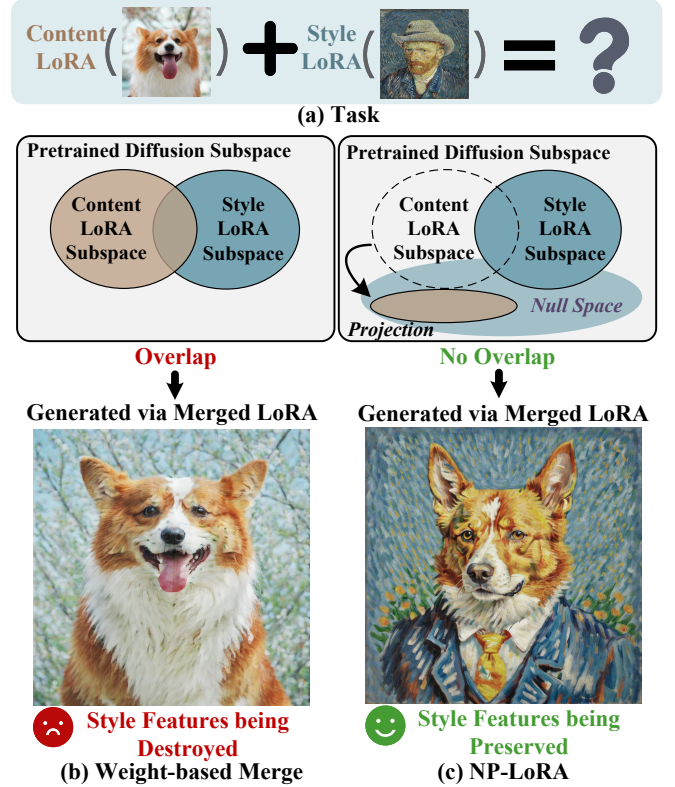


Fig. 1. Illustration of our motivation. (a) The task is to compose a content LoRA encoding subject identity with a style LoRA capturing artistic appearance for reusable and controllable generation. (b) Weighted LoRA merging degrades style fidelity due to interference: independently trained LoRAs occupy correlated, non-orthogonal low-rank subspaces in the shared diffusion feature space. (c) NP-LoRA projects the content LoRA into the null space of the style LoRA, eliminating subspace overlap and preserving stylistic features.

fusion ratio through loss optimization, K-LoRA [8] performs piecewise binary weight between the content and style LoRAs across diffusion timesteps, and LoRA.rar [9] predicts fusion weights via a pretrained hypernetwork. However, such weight-based merging methods inherently cause interference between the two LoRAs. As shown in Fig. 1(b), weighted addition of ΔW_c and ΔW_s distorts the style LoRA and degrades stylistic fidelity in generated images. This interference arises because independently trained LoRAs are optimized within the same feature space of the pretrained diffusion model, which leads them to occupy correlated low-rank subspaces and adapt similar feature dimensions (e.g., texture or color patterns). As a result, their low-rank subspaces inevitably overlap and become non-orthogonal. Moreover, empirical analysis (Sec. IV-A) re-

veals that LoRAs exhibit a structured low-rank space, where a few principal directions dominate generative behavior. These directions are highly sensitive to perturbations, indicating the need to explicitly preserve them during fusion. To address this issue, we reformulate the merging objective: rather than simply performing a weighted merge of ΔW_c and ΔW_s , the goal is to geometrically transform the content LoRA by projecting it into the null space of the style subspace.

To achieve this goal, we propose Null Space Projection LoRA (NP-LoRA), a projection-based framework that prevents interference between content and style LoRAs. Specifically, we perform singular value decomposition (SVD) on the style LoRA ΔW_s to extract its principal directions and define their orthogonal complement as a null space for interference-free fusion, as illustrated in Fig. 1(c). Based on this construction, we first formulate a strict projection scheme that projects the content LoRA ΔW_c fully onto the null space of the style LoRA to eliminate interference. This strict formulation completely removes style-interference effects, achieving a clear separation between content and style representations. Building on this foundation, we introduce a soft projection formulation that relaxes the hard projection into a continuous, tunable process. By modulating the projection strength with a single parameter, it adaptively suppresses interference while balancing subject fidelity and style consistency, effectively unifying both representations in LoRA fusion. The proposed NP-LoRA framework is fully training-free and applicable to a wide range of pretrained content-style LoRA pairs, offering a simple yet interpretable geometric view of LoRA fusion. Extensive experiments demonstrate that NP-LoRA consistently improves image fidelity and style coherence over strong baselines (e.g., DINO, CLIP-based, and human- and LLM-based preference metrics) across diverse backbones and LoRA combinations.

Our main contributions are summarized as follows:

- We propose Null Space Projection LoRA (NP-LoRA), a training-free projection-based geometric framework that unifies subject and style LoRAs through null space transformation.
- Our work applies SVD to explicitly resolve subspace overlap in LoRA merging by formulating LoRA fusion as a null-space projection problem. This approach removes interfering components by projection, enabling interference-free composition of independently trained LoRAs.
- We introduce a soft projection formulation that relaxes hard projection into a tunable process, adaptively suppressing interference and balancing subject fidelity and style consistency in LoRA fusion.
- We conduct extensive experiments demonstrating that NP-LoRA generalizes to diverse pretrained content-style LoRA pairs and consistently improves image fidelity and style coherence across strong baselines.

II. RELATED WORK

Customization and LoRA merging in diffusion models. Diffusion models [2], [3], [4], [5] have enabled extensive research on few-shot personalization. Early methods such as

Textual Inversion [10], [11], [12] and DreamBooth [6] capture subject identity by learning token embeddings or fine-tuning model parameters, while later approaches, including Custom Diffusion [13] and several training-free variants [14], [15], [16], [17], improve efficiency by reusing or selectively updating pretrained components. Low-Rank Adaptation (LoRA) [1], [18], [19], [20], [21], [22], [23], [24] provides a more efficient alternative via rank-decomposed adapters. Extensions such as B-LoRA [25] disentangle style and content for later fusion, while CSGO [26] composes content and style in a manner similar to image style transfer. Rather than jointly learning content and style, we focus on *merging independently trained LoRAs*. Existing LoRA merging methods for image generation can be broadly categorized into object composition [27], [28], [29], [30], [31], [32], [33] and content-style fusion [7], [8], [9], [34]. Recent methods such as ZipLoRA [7], K-LoRA [8], and LoRA.rar [9] move beyond naive addition through weighted fusion, adaptive switching, or hypernetworks. However, they all rely on weight-based merging and implicitly assume minimal interference between LoRAs, which our analysis shows to be flawed.

Orthogonality and Subspace Methods in Model Adaptation. Orthogonality is widely used in machine learning to reduce interference, often analyzed via singular value decomposition (SVD). Recent works [35], [36], [37], [38], [39] incorporate SVD or orthogonal designs in different adaptation settings and address distinct problems. KnOTS [35] uses SVD to extract shared bases for LoRA alignment and aggregation, but does not explicitly remove overlapping subspaces. SubZero [36] employs orthogonal cross-attention to mitigate content-style leakage during denoising, operating at the feature level rather than on LoRA parameters. LiON-LoRA [39] focuses on coordinating spatial-temporal LoRAs in video diffusion, rather than explicitly enforcing orthogonality via SVD-based projection. ProLoRA [37] and LoRA-Null [40] both exploit subspace or null-space properties of LoRA, but focus on LoRA re-adaptation or initialization rather than LoRA fusion. Although these methods leverage orthogonality or SVD, they target different scenarios and objectives. In contrast, we focus on LoRA merging by formulating LoRA fusion as a null-space projection problem and applying SVD to remove overlapping components by construction, enabling interference-free composition of independently trained LoRAs.

III. BACKGROUND

LoRA Fine-tuning. To efficiently adapt large diffusion models [2], [3], [4], [5] to specific concepts, Low-Rank Adaptation (LoRA) [1] has become a widely used fine-tuning technique. Instead of updating all pretrained parameters, LoRA inserts lightweight low-rank adapters into existing weight matrices. Given a pretrained weight $W_0 \in \mathbb{R}^{m \times n}$, the LoRA update is

$$\Delta W = BA, \quad B \in \mathbb{R}^{m \times r}, A \in \mathbb{R}^{r \times n}, \quad (1)$$

where $r \ll \min(m, n)$. Only A and B are optimized while W_0 remains frozen, greatly reducing memory and training cost. At inference, the adapted weight becomes

$$W = W_0 + \Delta W. \quad (2)$$

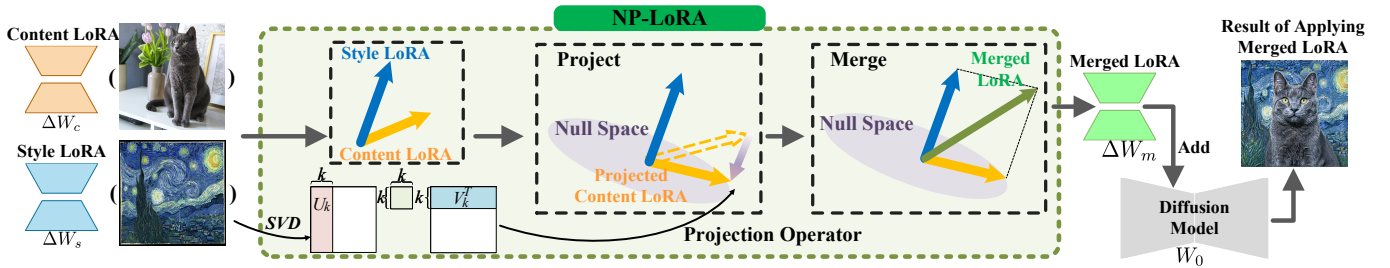


Fig. 2. Overview of the proposed method. NP-LoRA takes pretrained content and style LoRAs as inputs. The style LoRA is decomposed via singular value decomposition (SVD) to construct a null space, onto which the content LoRA is projected. This design enables effective fusion without extra training or hyperparameter tuning.

Once trained, LoRA modules can be directly applied to a diffusion backbone, conditioning it on new subjects or styles. **Problem Setup.** This work aims to merge two trained LoRAs, one for content and one for style, into a single LoRA that generates images faithful to both. We begin with a diffusion model containing pretrained weights $W_0^{(i)}$ and corresponding LoRA updates $\Delta W^{(i)}$. For simplicity, we omit the layer index (i) in subsequent formulations, as the same operation applies to all LoRA matrices [7]. We denote the content LoRA as ΔW_c , learned from images of a specific subject, and the style LoRA as ΔW_s , learned from images of a particular style. Our objective is to obtain a merged LoRA ΔW_m that integrates both content and style information:

$$\Delta W_m = \text{Merge}(\Delta W_c, \Delta W_s). \quad (3)$$

To achieve interference-free fusion, the merged LoRA must preserve the distinct characteristics of both content and style, motivating an analysis of how LoRA internally encodes and represents this information.

IV. METHODOLOGY

In this work, we present NP-LoRA, a training-free framework for fusing independently trained LoRAs, as illustrated in Fig. 2. We first perform singular value decomposition (SVD) to identify the principal directions of the style LoRA. A hard projection then maps the content LoRA onto the orthogonal complement of the style subspace, fully eliminating overlapping directions. To provide controllable flexibility, we further introduce a soft projection controlled by a tunable parameter, enabling smooth and adaptive fusion between content and style.

A. Principal Direction Extraction via SVD

We extract principal directions via singular value decomposition (SVD), decomposing the style LoRA weight as

$$\Delta W_s = U \Sigma V^\top, \quad (4)$$

where the columns of $V \in \mathbb{R}^{d_{in} \times r_s}$ are orthonormal right singular vectors. Each vector $v \in V$ defines a distinct direction in the parameter space, and its corresponding singular value in Σ quantifies the contribution strength of ΔW_s along that direction. Following the convention of K-LoRA [8], [6], all LoRAs are trained with rank 8; thus, we regard the top eight

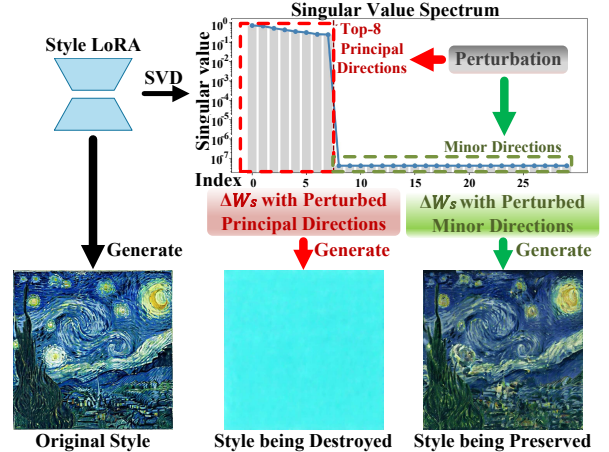


Fig. 3. Singular value spectrum of a LoRA and perturbation effects. We first visualize the singular value spectrum, then perturb the principal and minor directions respectively. Perturbations on principal directions destroy style consistency, whereas those on minor directions have little impact.

singular vectors (those with the largest singular values) as the principal directions. To investigate their impact, we visualize the generative effects of perturbing these directions. As shown in Fig. 3, perturbing dominant components causes a sharp drop in stylistic consistency, whereas perturbing minor ones yields minimal change, confirming that these principal directions play a critical role in generation fidelity.

Having identified the principal style directions that should be preserved, we next examine whether existing weight-based merging can protect them. A straightforward combination of content and style LoRAs takes the form

$$\Delta W_m = a \Delta W_c + b \Delta W_s, \quad a, b \in \mathbb{R}. \quad (5)$$

However, such linear fusion fails to prevent interference with the style-critical subspace introduced by the content LoRA, as shown in Fig. 5 (c).

Proposition 1. *Given content LoRA ΔW_c and style LoRA ΔW_s , their weighted combination cannot, in general, isolate the content feature from the style-critical subspace. As a result, content-induced interference is unavoidable, and stylistic consistency cannot be guaranteed.*

Proof: Let the style subspace be spanned by the top singular vectors of ΔW_s , denoted by V_k , and define the

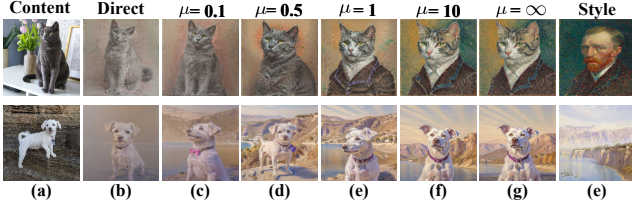


Fig. 4. (a) and (e) are the content and style references, respectively. (c) shows the result of direct merging, which corresponds to $\mu = 0$ (i.e., the degenerate case of NP-LoRA). (d)-(g) show results for $\mu = 0.1, 0.5, 1, 10$, and ∞ , where $\mu = \infty$ represents the hard projection case of our method. Small μ values cause content-style interference, whereas large μ values preserve style at the expense of content fidelity.

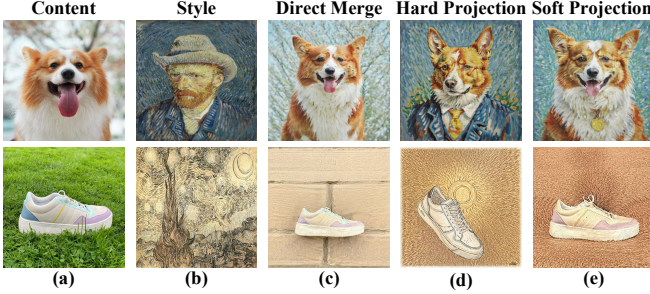


Fig. 5. Visualization of our method. (a) Content image. (b) Style image. (c) Results of direct weight-based merging, which causes style distortion and interference. (d) Results of hard projection (the base formulation of our method), which removes interference but suppresses content details. (e) Results of soft projection (ours), achieving a balanced fusion of subject fidelity and style consistency.

projection operator $P = V_k V_k^\top$. Decomposing the content LoRA yields

$$\Delta W_c = (I - P)\Delta W_c + P\Delta W_c, \quad (6)$$

where $P\Delta W_c$ lies in the style subspace. For a weighted merge $\Delta W_m = a\Delta W_c + b\Delta W_s$, its projection onto the style subspace is

$$P\Delta W_m = aP\Delta W_c + b\Delta W_s. \quad (7)$$

To preserve the original style component, we require $P\Delta W_m = \Delta W_s$, implying

$$aP\Delta W_c = (1 - b)\Delta W_s. \quad (8)$$

This condition admits a solution only if $P\Delta W_c$ and ΔW_s are colinear (i.e., $P\Delta W_c = \alpha\Delta W_s$), which is almost never the case for independently trained LoRAs. Even with vectorized weights a, b , each column of $P\Delta W_c$ must lie in the span of ΔW_s , which is statistically improbable in high-dimensional space. Hence, weighted merging inevitably introduces interference within the style subspace, leading to style degradation. ■

B. Hard Projection for Subspace Separation

Having identified the principal style directions that must be preserved and shown that weight-based merging fails to protect them, we now introduce our projection-based formulation. We inject the content LoRA into the style LoRA, as style representations are inherently more fragile and easily over-

written than structural or semantic features [41], [42], [43]. As demonstrated in Sec. V-D, this design preserves stylistic consistency while retaining content-specific information.

We define the orthogonal projection onto the null space of the style subspace:

$$P_{\text{null}} = I - V_k V_k^\top, \quad (9)$$

where I denotes the identity matrix. This operator removes any component aligned with the protected style directions, retaining only the part that is orthogonal to them. Applying this projection to the content LoRA ΔW_c yields the style-orthogonal component:

$$\Delta W_c^\perp = \Delta W_c P_{\text{null}}. \quad (10)$$

The merged LoRA is defined as

$$\begin{aligned} \Delta W_m &= \Delta W_s + \Delta W_c^\perp \\ &= \Delta W_s + \Delta W_c (I - V_k V_k^\top). \end{aligned} \quad (11)$$

This construction ensures that the content LoRA ΔW_c contributes only through directions orthogonal to the style subspace, leaving the principal style directions exclusively governed by ΔW_s , as shown in Fig. 5 (d).

Proposition 2. *By applying Eq. 11, the proposed projection-based merging ensures that only style-orthogonal content information is injected. Consequently, no content-induced interference can occur within the protected style subspace.*

Proof: For any input x , the projected content LoRA is

$$\Delta W_c^\perp x = \Delta W_c P_{\text{null}} x. \quad (12)$$

To verify that it does not intrude into the style-critical subspace, we examine its projection onto it:

$$\begin{aligned} P(\Delta W_c^\perp x) &= P \Delta W_c P_{\text{null}} x \\ &= V_k V_k^\top \Delta W_c (I - V_k V_k^\top) x. \end{aligned} \quad (13)$$

Since $V_k^\top V_k = I_k$, it follows that

$$V_k V_k^\top (I - V_k V_k^\top) = 0, \quad (14)$$

which immediately yields

$$P(\Delta W_c^\perp x) = 0. \quad (15)$$

Thus, $\Delta W_c^\perp x$ has no component in $\text{span}(V_k)$ and is completely orthogonal to the style-critical subspace. ■

This confirms that $\Delta W_c^\perp x$ lies entirely in the orthogonal complement of the style subspace, ensuring that the style-critical directions governed by ΔW_s remain unaffected. From an energy perspective, this means that the contribution of the content LoRA within the style subspace is suppressed. We quantify this residual interaction by the following quadratic form:

$$(\Delta W_c^{\text{proj}})^\top P \Delta W_c^{\text{proj}}, \quad (16)$$

which measures the remaining energy of ΔW_c^{proj} along the style subspace. The hard projection in Eq. 10 minimizes this energy, effectively driving style interference to zero.

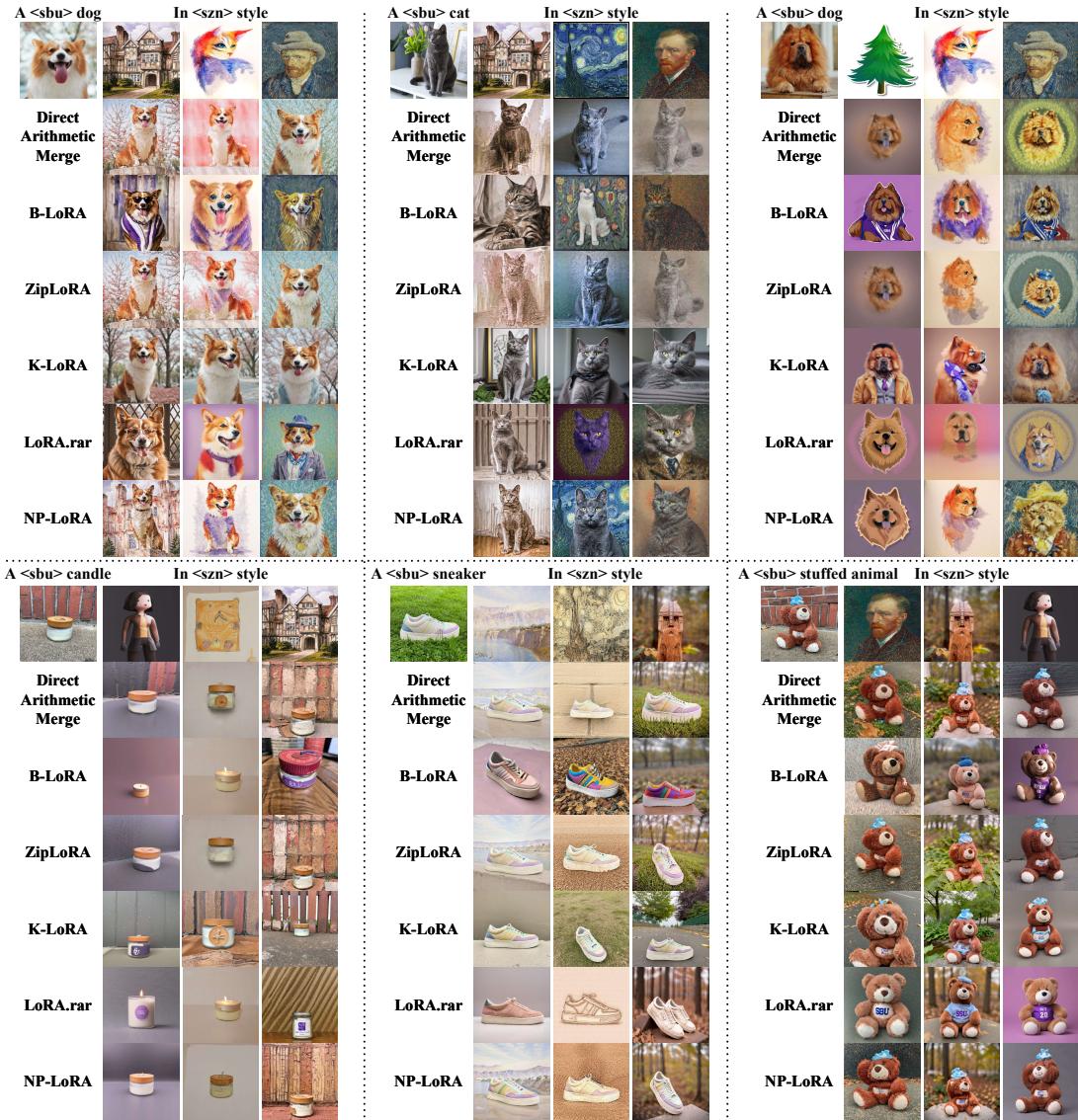


Fig. 6. Qualitative comparison with Direct Weight Merge, B-LoRA, ZipLoRA, K-LoRA, LoRA.rar, and our proposed NP-LoRA, illustrating the trade-off between subject fidelity and style preservation.

C. Soft Projection for Balanced Fusion

While hard projection achieves perfect style preservation, it also removes content features that partially align with style directions, as shown in Fig. 5 (d). As a result, the projection becomes overly conservative, motivating the need for a more flexible alternative. We therefore introduce a relaxed formulation that balances style preservation and content retention. Specifically, we consider a Tikhonov-regularized [44] variant of the previous objective:

$$\min_{\Delta W_c^{\text{proj}}} \|\Delta W_c^{\text{proj}} - \Delta W_c\|_2^2 + \mu (\Delta W_c^{\text{proj}})^\top P \Delta W_c^{\text{proj}}, \quad (17)$$

where the first term encourages closeness to the original content LoRA ΔW_c , and the second penalizes the energy retained within the style subspace, with $\mu \geq 0$ controlling the suppression strength.

Taking the derivative and setting it to zero gives

$$\Delta W_c^{\text{proj}} = (I + \mu P)^{-1} \Delta W_c. \quad (18)$$

Since $P = V_k V_k^\top$ with $V_k^\top V_k = I_k$, the inverse admits a simple closed form derived from the Woodbury identity [45] (see Supplementary Material for a detailed derivation):

$$(I + \mu P)^{-1} = I - \frac{\mu}{1 + \mu} V_k V_k^\top. \quad (19)$$

This yields the soft projection operator and the projected content LoRA:

$$P_{\text{soft}} = I - \frac{\mu}{1 + \mu} V_k V_k^\top, \quad \Delta W_c^{\text{proj}} = P_{\text{soft}} \Delta W_c. \quad (20)$$

Finally, the merged LoRA is

$$\begin{aligned} \Delta W_m &= \Delta W_s + \Delta W_c^{\text{proj}} \\ &= \Delta W_s + (I - \frac{\mu}{1 + \mu} V_k V_k^\top) \Delta W_c. \end{aligned} \quad (21)$$

This formulation explicitly separates the two components:

the part of ΔW_c outside the style subspace is preserved, while the overlapping style-interference part is attenuated by a factor of $\frac{\mu}{1+\mu}$. By adjusting the parameter μ , our method provides a continuous spectrum from linear merging ($\mu \rightarrow 0$) to strict orthogonal projection ($\mu \rightarrow \infty$). In this way, NP-LoRA achieves balanced fusion that maintains stylistic consistency without compromising content semantics, as shown in Fig. 5(e).

V. EXPERIMENTS

A. Experiment Setup

Datasets. Following common practice in customization [7], [8], we obtain LoRAs from publicly available images. For content, we adopt the DreamBooth [46] dataset, where each subject is represented by 4–5 reference images. For style, we use the StyleDrop [47] dataset, complemented with several representative artistic styles. For community-trained LoRAs, we use publicly available models from Hugging Face for evaluation.

Experimental details. All experiments are conducted on the SDXL v1.0 [48]. For training the LoRAs to be merged, including the training prompts and ranks, we follow the settings in K-LoRA [8], [6]. The key hyperparameter μ in the soft projection (Eq. 21) is fixed to 0.5, with a detailed analysis provided in Sec. V-B. Implementation details are provided in the supplemental material. Experiments based on SDXL are performed on an NVIDIA RTX 3090 GPU.

Baselines. We compare our method with representative approaches for combining or learning multiple LoRAs. Among them, most methods merge two independently trained LoRAs, i.e., the model takes two trained LoRAs as input and produces merged generations. Specifically, we evaluate (i) the direct weight merging baseline $\Delta W_m = \Delta W_c + \Delta W_s$, (ii) B-LoRA [25] (ECCV2024), (iii) ZipLoRA [7] (ECCV2024), (iv) K-LoRA [8] (CVPR2025), and (v) LoRA.rar [9] (ICCV2025).

B. Ablation on Projection Strength

We analyze the effect of the projection strength controlled by the parameter μ , which balances subject fidelity and style consistency, as shown in Fig. 4. As μ increases from 0 to ∞ , the projection strength grows: when $\mu \rightarrow 0$, NP-LoRA reduces to direct weight-based merging dominated by the content LoRA, yet leading to content-style interference, and as $\mu \rightarrow \infty$, it approaches a hard projection that removes content components overlapping with the style subspace. We evaluate NP-LoRA across $\mu \in \{0, 0.1, 0.5, 1, 10, \infty\}$ to study this transition. This ablation reveals a clear trade-off: small μ values lead to content-style interference, while large μ values preserve style but suppress content details. In particular, the hard projection ($\mu = \infty$) loses rich content features, confirming the necessity of the soft projection mechanism. Empirically, $\mu = 0.5$ yields the best balance and is used as the default in all subsequent experiments. Additional qualitative and quantitative results are provided in the Supplementary Material.

TABLE I
COMPARISON OF METHODS USING CLIP AND DINO SIMILARITIES FOR CONTENT AND STYLE. THE AGGREGATED SCORES (S_{ARITH} , S_{HARM}) SUMMARIZE THE OVERALL CONTENT-STYLE TRADE-OFF.

Method	$S_{\text{content}}^{\text{CLIP}}$	$S_{\text{style}}^{\text{CLIP}}$	$S_{\text{content}}^{\text{DINO}}$	$S_{\text{style}}^{\text{DINO}}$	S_{arith}	S_{harm} \uparrow
Direct	0.75	0.55	0.54	0.23	0.51	0.42
B-LoRA	0.72	0.55	0.51	0.26	0.51	0.44
ZipLoRA	0.75	0.56	0.55	0.24	0.52	0.44
K-LoRA	0.76	0.55	0.57	0.22	0.52	0.42
LoRA.rar	0.70	0.53	0.50	0.30	0.51	0.46
NP-LoRA	0.73	0.59	0.52	0.33	0.55	0.50

TABLE II
USER PREFERENCE AND GPT-5 EVALUATION COMPARISON. BOTH HUMAN USERS AND GPT-5 ARE ASKED TO SELECT THE BEST RESULT AMONG THE CANDIDATES. THE REPORTED SCORE REPRESENTS THE PROPORTION OF CASES WHERE EACH METHOD IS SELECTED AS THE BEST.

Method	User Preference \uparrow	GPT5 Feedback \uparrow
Direct	7.97%	6.25%
B-LoRA	9.06%	9.38%
ZipLoRA	10.00%	9.38%
K-LoRA	12.19%	12.50%
LoRA.rar	11.25%	9.38%
NP-LoRA	49.53%	53.13%

C. Results

a) Quantitative comparisons.: In order to ensure a fair evaluation, all experiments at this stage are conducted using SDXL. Following prior works including K-LoRA [8] (18 pairs) and ZipLoRA [7] (32 pairs), we evaluate our NP-LoRA on 32 randomly selected content-style LoRA pairs, covering 5 animal subjects, 5 object-level categories, and 15 distinct artistic styles. Each pair contains 10 generated images, which will be clarified in Supplementary Material. For evaluation, following prior work [7], [8], we adopt CLIP [49] and DINO [50] similarity metrics to jointly assess subject preservation (content) and style alignment (style) [51], [7], [8]. These metrics are widely used in the literature on LoRA merging. Specifically, for CLIP we compute $S_{\text{content}}^{\text{CLIP}}$ and $S_{\text{style}}^{\text{CLIP}}$, and for DINO we compute $S_{\text{content}}^{\text{DINO}}$ and $S_{\text{style}}^{\text{DINO}}$. To obtain unified content-style similarity measures, we report both the arithmetic mean and the harmonic mean following the common F1-style aggregation scheme [52], [53], [54], [55]. Given the four similarity scores $S_i \in \{S_{\text{content}}^{\text{CLIP}}, S_{\text{style}}^{\text{CLIP}}, S_{\text{content}}^{\text{DINO}}, S_{\text{style}}^{\text{DINO}}\}$, we report both the arithmetic mean $S_{\text{arith}} = \frac{1}{4} \sum_i S_i$ and the harmonic mean $S_{\text{harm}} = \frac{4}{\sum_i (1/S_i)}$, where S_{arith} reflects the overall trend, while the harmonic mean S_{harm} emphasizes joint fidelity to both content and style. As shown in Tab. I, our method achieves the highest S_{arith} and S_{overall} , showing its superior ability to balance subject fidelity and style consistency.

Following K-LoRA [8], we further evaluated perceptual quality through a user study involving 20 participants. The study was conducted on images generated from 32 merged LoRA pairs (Tab. I), with 32 images sampled from each pair. Each case included outputs from SOTA baselines and

TABLE III

EFFICIENCY COMPARISON OF DIFFERENT LoRA MERGING STRATEGIES. MERGE (s^\dagger) INCLUDES MODEL LOADING TIME; GEN./IMG. (s) IS THE AVERAGE GENERATION TIME PER IMAGE. LoRA.RAR [9] IS EXCLUDED FOR ITS NEEDS PRETRAINED MODELS, AND B-LoRA [25] IS OMITTED FOR REQUIRING SCRATCH TRAINING.

Method	Merge (s^\dagger) ↓	Gen./Img. (s) ↓
Direct	13.466	22.898
ZipLoRA	> 10 min	29.931
K-LoRA	12.250*	60.388*
NP-LoRA	13.440	23.208

* Only includes LoRA loading time, as K-LoRA performs on-the-fly merging during generation.

our method, along with reference subject and style images. Participants selected the result best balancing subject fidelity and style consistency. As shown in Tab. II, our method was preferred in 49.53% of cases. We further adopted a GPT-5-based automatic evaluation protocol, which is more recent than the MLLM evaluator used in [9]. The results show a consistent 53.13% preference in favor of our method.

b) Qualitative comparisons.: Qualitative results are shown in Fig. 6. Direct merging and ZipLoRA [7] achieve partial fusion but often fail on certain content-style pairs. B-LoRA [25] captures style traits, but compromises on the content fidelity. K-LoRA [8] preserves subject identity well yet struggles to capture the desired style, while LoRA.rar [9] delivers only marginal improvements but still falls short. In contrast, NP-LoRA achieves the best results, achieving a superior balance between content fidelity and style preservation. A qualitative comparison with jointly training method in the Supplementary Material shows that NP-LoRA attains superior results.

c) Efficiency Comparison.: To evaluate efficiency, we compare both the merging and generation times in Tab. III. LoRA.rar [9] is excluded because it depends on pretrained models for parameter fusion, and B-LoRA [25] is also omitted since it requires training from scratch instead of merging pretrained LoRAs. ZipLoRA [7] is the slowest due to additional fusion optimization, whereas K-LoRA [8] is efficient during initialization but slows down for dynamic fusion in the sampling stage. In contrast, NP-LoRA maintains merging and inference efficiency comparable to Direct Merge baseline, yet consistently delivers superior results.

D. Projection Direction: Content into Style

As shown in Fig. 6 and Tab. I, direct merging overwhelmingly favors the content LoRA: structural information is preserved while stylistic traits are largely lost. The projection in Fig. 7 further confirms that embedding style into the content space almost fully erases style signals. This suggests that content representations are inherently more dominant and resistant to interference, whereas style features are fragile. Therefore, we reverse the direction of projection and map the content LoRA onto the null space of the style LoRA, injecting content only along interference-free directions. This

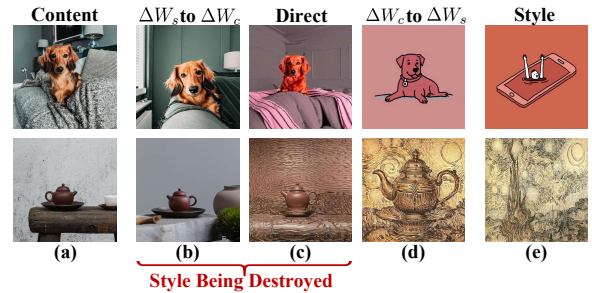


Fig. 7. Comparison of LoRA Projection. (a) Content LoRA training images, (b) style LoRA projected into the content LoRA null space, (c) direct merge, (d) content LoRA projected into the style LoRA null space, and (e) style LoRA training images. (b) and (c) degrade style consistency, with (b) almost removing stylistic traits, while (d) better balances content and style.

preserves stylistic consistency while still retaining content-specific information.

VI. CONCLUSIONS

In this paper, we propose NP-LoRA, a merging strategy that harmoniously unifies style and content LoRAs while avoiding destructive interference. NP-LoRA identifies a style-critical subspace via SVD and projects the content LoRA onto its orthogonal complement, followed by soft attenuation of overlapping components to control flexibility. We further provide theoretical analysis explaining the failure of conventional weight merging and the effectiveness of null-space projection. Extensive experiments, including quantitative metrics, user studies, and GPT-5 evaluations, demonstrate the effectiveness of NP-LoRA, which achieves significant performance gains with runtime efficiency comparable to direct merging.

Limitations. Our method assumes cross-layer independence of LoRA representations, as in prior merging approaches [7], [8], [9], which may miss complex cross-layer or non-linear dependencies. In addition, the attenuation coefficient μ in NP-LoRA is empirically set, and we leave adaptive or data-driven selection for future work.

REFERENCES

- [1] E. J. Hu, Y. Shen, P. Wallis, Z. Allen-Zhu, Y. Li, S. Wang, L. Wang, W. Chen, *et al.*, “Lora: Low-rank adaptation of large language models.” *ICLR*, vol. 1, no. 2, p. 3, 2022.
- [2] J. Ho, A. Jain, and P. Abbeel, “Denoising diffusion probabilistic models,” *Advances in Neural Information Processing Systems*, vol. 33, pp. 6840–6851, 2020.
- [3] J. Song, C. Meng, and S. Ermon, “Denoising diffusion implicit models,” in *International Conference on Learning Representations*, 2021. [Online]. Available: <https://openreview.net/forum?id=St1giarCHLP>
- [4] P. Dhariwal and A. Nichol, “Diffusion models beat gans on image synthesis,” in *Advances in Neural Information Processing Systems*, M. Ranzato, A. Beygelzimer, Y. Dauphin, P. Liang, and J. W. Vaughan, Eds., vol. 34. Curran Associates, Inc., 2021, pp. 8780–8794. [Online]. Available: https://proceedings.neurips.cc/paper_files/paper/2021/file/49ad23d1ec9fa4bd8d77d02681df5cfa-Paper.pdf
- [5] R. Rombach, A. Blattmann, D. Lorenz, P. Esser, and B. Ommer, “High-resolution image synthesis with latent diffusion models,” in *Proceedings of the IEEE/CVF Conference on Computer Vision and Pattern Recognition (CVPR)*, June 2022, pp. 10 684–10 695.
- [6] N. Ruiz, Y. Li, V. Jampani, Y. Pritch, M. Rubinstein, and K. Aberman, “Dreambooth: Fine tuning text-to-image diffusion models for subject-driven generation,” in *Proceedings of the IEEE/CVF conference on computer vision and pattern recognition*, 2023, pp. 22 500–22 510.

- [7] V. Shah, N. Ruiz, F. Cole, E. Lu, S. Lazebnik, Y. Li, and V. Jampani, “Ziplora: Any subject in any style by effectively merging loras,” in *European Conference on Computer Vision*. Springer, 2024, pp. 422–438.
- [8] Z. Ouyang, Z. Li, and Q. Hou, “K-lora: Unlocking training-free fusion of any subject and style loras,” in *CVPR*, 2025.
- [9] D. Shenaj, O. Bohdal, M. Ozay, P. Zanuttigh, and U. Michieli, “Lora.rar: Learning to merge loras via hypernetworks for subject-style conditioned image generation,” in *Proceedings of the IEEE/CVF International Conference on Computer Vision (ICCV)*, October 2025.
- [10] Y. Alaluf, E. Richardson, G. Metzger, and D. Cohen-Or, “A neural space-time representation for text-to-image personalization,” *ACM Transactions on Graphics (TOG)*, vol. 42, no. 6, pp. 1–10, 2023.
- [11] A. Voynov, Q. Chu, D. Cohen-Or, and K. Aberman, “p+: Extended textual conditioning in text-to-image generation,” *arXiv preprint arXiv:2303.09522*, 2023.
- [12] Y. Zhang, N. Huang, F. Tang, H. Huang, C. Ma, W. Dong, and C. Xu, “Inversion-based style transfer with diffusion models,” in *Proceedings of the IEEE/CVF conference on computer vision and pattern recognition*, 2023, pp. 10 146–10 156.
- [13] N. Kumari, B. Zhang, R. Zhang, E. Shechtman, and J.-Y. Zhu, “Multi-concept customization of text-to-image diffusion,” in *Proceedings of the IEEE/CVF conference on computer vision and pattern recognition*, 2023, pp. 1931–1941.
- [14] O. Avrahami, K. Aberman, O. Fried, D. Cohen-Or, and D. Lischinski, “Break-a-scene: Extracting multiple concepts from a single image,” in *SIGGRAPH Asia 2023 Conference Papers*, 2023, pp. 1–12.
- [15] J. Shi, W. Xiong, Z. Lin, and H. J. Jung, “Instantbooth: Personalized text-to-image generation without test-time finetuning,” in *Proceedings of the IEEE/CVF conference on computer vision and pattern recognition*, 2024, pp. 8543–8552.
- [16] G. Xiao, T. Yin, W. T. Freeman, F. Durand, and S. Han, “Fastcomposer: Tuning-free multi-subject image generation with localized attention,” *International Journal of Computer Vision*, vol. 133, no. 3, pp. 1175–1194, 2025.
- [17] S. Xie, Z. Zhang, Z. Lin, T. Hinz, and K. Zhang, “Smartbrush: Text and shape guided object inpainting with diffusion model,” in *Proceedings of the IEEE/CVF conference on computer vision and pattern recognition*, 2023, pp. 22 428–22 437.
- [18] S. Hayou, N. Ghosh, and B. Yu, “Lora+: Efficient low rank adaptation of large models,” *arXiv preprint arXiv:2402.12354*, 2024.
- [19] D. J. Kopiczko, T. Blankevoort, and Y. M. Asano, “Vera: Vector-based random matrix adaptation,” *arXiv preprint arXiv:2310.11454*, 2023.
- [20] P. Ren, C. Shi, S. Wu, M. Zhang, Z. Ren, M. de Rijke, Z. Chen, and J. Pei, “Melora: Mini-ensemble low-rank adapters for parameter-efficient fine-tuning,” *arXiv preprint arXiv:2402.17263*, 2024.
- [21] L. Zhang, L. Zhang, S. Shi, X. Chu, and B. Li, “Lora-fa: Memory-efficient low-rank adaptation for large language models fine-tuning,” *arXiv preprint arXiv:2308.03303*, 2023.
- [22] H. Zhou, X. Lu, W. Xu, C. Zhu, T. Zhao, and M. Yang, “Lora-drop: Efficient lora parameter pruning based on output evaluation,” *arXiv preprint arXiv:2402.07721*, 2024.
- [23] B. Zi, X. Qi, L. Wang, J. Wang, K.-F. Wong, and L. Zhang, “Delta-lora: Fine-tuning high-rank parameters with the delta of low-rank matrices,” *arXiv preprint arXiv:2309.02411*, 2023.
- [24] A. Roy, S. Borse, S. Kadambi, D. Das, S. Mahajan, R. Garrepalli, H. Park, A. Nayak, R. Chellappa, M. Hayat, and F. Porikli, “Duolora: Cycle-consistent and rank-disentangled content-style personalization,” in *Proceedings of the IEEE/CVF International Conference on Computer Vision (ICCV)*, October 2025, pp. 15 395–15 404.
- [25] Y. Frenkel, Y. Vinker, A. Shamir, and D. Cohen-Or, “Implicit style-content separation using b-lora,” in *European Conference on Computer Vision*. Springer, 2024, pp. 181–198.
- [26] P. Xing, H. Wang, Y. Sun, Q. Wang, X. Bai, H. Ai, R. Huang, and Z. Li, “Csgo: Content-style composition in text-to-image generation,” *arXiv preprint arXiv:2408.16766*, 2024.
- [27] J. Dong, W. Liang, H. Li, D. Zhang, M. Cao, H. Ding, S. H. Khan, and F. Shahbaz Khan, “How to continually adapt text-to-image diffusion models for flexible customization?” *Advances in Neural Information Processing Systems*, vol. 37, pp. 130 057–130 083, 2024.
- [28] Y. Gu, X. Wang, J. Z. Wu, Y. Shi, Y. Chen, Z. Fan, W. Xiao, R. Zhao, S. Chang, W. Wu, et al., “Mix-of-show: Decentralized low-rank adaptation for multi-concept customization of diffusion models,” *Advances in Neural Information Processing Systems*, vol. 36, pp. 15 890–15 902, 2023.
- [29] J. Jiang, Y. Zhang, K. Feng, X. Wu, W. Li, R. Pei, F. Li, and W. Zuo, “Mc²: Multi-concept guidance for customized multi-concept generation,” in *Proceedings of the Computer Vision and Pattern Recognition Conference*, 2025, pp. 2802–2812.
- [30] Z. Liu, R. Feng, K. Zhu, Y. Zhang, K. Zheng, Y. Liu, D. Zhao, J. Zhou, and Y. Cao, “Cones: Concept neurons in diffusion models for customized generation,” *arXiv preprint arXiv:2303.05125*, 2023.
- [31] Y. Yang, W. Wang, L. Peng, C. Song, Y. Chen, H. Li, X. Yang, Q. Lu, D. Cai, B. Wu, et al., “Lora-composer: Leveraging low-rank adaptation for multi-concept customization in training-free diffusion models,” *arXiv preprint arXiv:2403.11627*, 2024.
- [32] M. Zhong, Y. Shen, S. Wang, Y. Lu, Y. Jiao, S. Ouyang, D. Yu, J. Han, and W. Chen, “Multi-lora composition for image generation,” *Transactions on Machine Learning Research*, vol. 2024, 2024.
- [33] A. Zhang, X. Ding, H. Wang, S. McDonagh, and S. Kaski, “Rethinking inter-lora orthogonality in adapter merging: Insights from orthogonal monte carlo dropout,” *arXiv preprint arXiv:2510.03262*, 2025.
- [34] J.-C. Zhang and Y.-J. Xiong, “Subject or style: Adaptive and training-free mixture of loras,” *arXiv preprint arXiv:2508.02165*, 2025.
- [35] G. Stoica, P. Ramesh, B. Ecsedi, L. Choshen, and J. Hoffman, “Model merging with svd to tie the knots,” in *The Thirteenth International Conference on Learning Representations*.
- [36] S. Borse, K. Bhardwaj, M. R. K. Dastjerdi, H. Park, S. Kadambi, S. Shivakumar, P. Mandke, A. Nayak, H. Teague, M. Hayat, et al., “Subzero: Composing subject, style, and action via zero-shot personalization,” *arXiv preprint arXiv:2502.19673*, 2025.
- [37] F. Farhadzadeh, D. Das, S. Borse, and F. Porikli, “Zero-shot adaptation of parameter-efficient fine-tuning in diffusion models,” in *Proceedings of the 42nd International Conference on Machine Learning*, ser. Proceedings of Machine Learning Research, A. Singh, M. Fazel, D. Hsu, S. Lacoste-Julien, F. Berkenkamp, T. Maharaj, K. Wagstaff, and J. Zhu, Eds., vol. 267. PMLR, 13–19 Jul 2025, pp. 16 144–16 160. [Online]. Available: <https://proceedings.mlr.press/v267/farhadzadeh25a.html>
- [38] J. Fang, H. Jiang, K. Wang, Y. Ma, J. Shi, X. Wang, X. He, and T.-S. Chua, “Alphaedit: Null-space constrained knowledge editing for language models,” in *The Thirteenth International Conference on Learning Representations*.
- [39] Y. Zhang, C. Cao, C. Yu, and J. Zhu, “Lion-lora: Rethinking lora fusion to unify controllable spatial and temporal generation for video diffusion,” in *Proceedings of the IEEE/CVF International Conference on Computer Vision*, 2025, pp. 14 569–14 579.
- [40] P. Tang, Y. Liu, D. Zhang, X. Wu, and D. Zhang, “Lora-null: Low-rank adaptation via null space for large language models,” *arXiv preprint arXiv:2503.02659*, 2025.
- [41] L. A. Gatys, A. S. Ecker, and M. Bethge, “Image style transfer using convolutional neural networks,” in *Proceedings of the IEEE conference on computer vision and pattern recognition*, 2016, pp. 2414–2423.
- [42] X. Huang and S. Belongie, “Arbitrary style transfer in real-time with adaptive instance normalization,” in *Proceedings of the IEEE international conference on computer vision*, 2017, pp. 1501–1510.
- [43] Y. Li, C. Fang, J. Yang, Z. Wang, X. Lu, and M.-H. Yang, “Universal style transfer via feature transforms,” *Advances in neural information processing systems*, vol. 30, 2017.
- [44] A. Tikhonov and V. Arsenin, *Solutions of Ill-posed Problems*, ser. Halsted Press book. Winston, 1977. [Online]. Available: <https://books.google.co.jp/books?id=ECrvAAAAMAAJ>
- [45] M. Woodbury and P. U. D. of Statistics, *Inverting Modified Matrices*, ser. Memorandum Report / Statistical Research Group, Princeton. Department of Statistics, Princeton University, 1950. [Online]. Available: https://books.google.co.jp/books?id=_zAnzgEACAAJ
- [46] N. Ruiz, Y. Li, V. Jampani, Y. Pritch, M. Rubinstein, and K. Aberman, “Dreambooth: Fine tuning text-to-image diffusion models for subject-driven generation,” in *Proceedings of the IEEE/CVF conference on computer vision and pattern recognition*, 2023, pp. 22 500–22 510.
- [47] K. Sohn, N. Ruiz, K. Lee, D. C. Chin, I. Blok, H. Chang, J. Barber, L. Jiang, G. Entis, Y. Li, et al., “Styldrop: Text-to-image generation in any style,” *arXiv preprint arXiv:2306.00983*, 2023.
- [48] D. Podell, Z. English, K. Lacey, A. Blattmann, T. Dockhorn, J. Müller, J. Penna, and R. Rombach, “Sdxl: Improving latent diffusion models for high-resolution image synthesis,” *arXiv preprint arXiv:2307.01952*, 2023.
- [49] A. Radford, J. W. Kim, C. Hallacy, A. Ramesh, G. Goh, S. Agarwal, G. Sastry, A. Askell, P. Mishkin, J. Clark, G. Krueger, and I. Sutskever, “Learning transferable visual models from natural language supervision,” in *Proceedings of the 38th International Conference on Machine Learning*, ser. Proceedings of Machine Learning Research, M. Meila and T. Zhang, Eds., vol. 139.

- PMLR, 18–24 Jul 2021, pp. 8748–8763. [Online]. Available: <https://proceedings.mlr.press/v139/radford21a.html>
- [50] H. Zhang, F. Li, S. Liu, L. Zhang, H. Su, J. Zhu, L. M. Ni, and H.-Y. Shum, “Dino: Detr with improved denoising anchor boxes for end-to-end object detection,” *arXiv preprint arXiv:2203.03605*, 2022.
- [51] D. Jiang, Y. Liu, S. Liu, J. Zhao, H. Zhang, Z. Gao, X. Zhang, J. Li, and H. Xiong, “From clip to dino: Visual encoders shout in multi-modal large language models,” 2024. [Online]. Available: <https://arxiv.org/abs/2310.08825>
- [52] C. Van Rijsbergen, *Information Retrieval*. Butterworths, 1979. [Online]. Available: <https://books.google.co.jp/books?id=t-pTAAAAMAAJ>
- [53] N. Chinchor, “Muc-4 evaluation metrics,” in *Proceedings of the 4th Conference on Message Understanding*, ser. MUC4 ’92. USA: Association for Computational Linguistics, 1992, p. 22–29. [Online]. Available: <https://doi.org/10.3115/1072064.1072067>
- [54] E. Ristani, F. Solera, R. Zou, R. Cucchiara, and C. Tomasi, “Performance measures and a data set for multi-target, multi-camera tracking,” in *Proceedings of the European Conference on Computer Vision (ECCV) Workshops*, 2016, pp. 17–35, proposes IDF1, a harmonic mean of ID precision and recall for tracking evaluation.
- [55] Y. Xian, C. H. Lampert, B. Schiele, and Z. Akata, “Zero-shot learning – the good, the bad and the ugly,” in *Proceedings of the IEEE Conference on Computer Vision and Pattern Recognition (CVPR)*, 2017, pp. 4582–4591, introduces the harmonic mean (H-score) of seen/unseen accuracies for balanced evaluation in generalized zero-shot learning.

SUPPLEMENTARY MATERIAL OVERVIEW

This supplementary material provides additional technical details, derivations, and extended analyses to support the findings presented in the main paper. Specifically, we first derive the formulation of the proposed soft projection operator in Sec. VII and present details for efficient implementation in Sec. IX. Sec. X investigates which null-space construction (U-space or V-space) better preserves stylistic fidelity. Sec. XII provides an additional comparison with joint training to further validate the effectiveness of NP-LoRA over training-based approaches. Sec. XIII demonstrates the controllability of our method under various prompt conditions, while Sec. XIV evaluates its robustness across different random seeds. Sec. XV extends our validation to the Flux model to assess cross-model generalization. Finally, Sec. XVI details the GPT-5 evaluation protocol used for quantitative preference assessment.

Together, these sections offer deeper insights into NP-LoRA’s formulation, implementation, and empirical robustness beyond the main paper.

VII. DERIVATION OF THE SOFT PROJECTION OPERATOR

We start from the relaxed objective introduced in the main text of our paper:

$$\min_{\Delta W_c^{\text{proj}}} \|\Delta W_c^{\text{proj}} - \Delta W_c\|_2^2 + \mu (\Delta W_c^{\text{proj}})^\top P \Delta W_c^{\text{proj}}, \quad (22)$$

where the first term preserves proximity to the original content adapter, and the second penalizes its activation within the style subspace defined by $P = V_k V_k^\top$.

a) Closed-form solution.: Taking the derivative of (22) with respect to ΔW_c^{proj} and setting it to zero gives

$$(I + \mu P) \Delta W_c^{\text{proj}} = \Delta W_c, \quad (23)$$

hence

$$\Delta W_c^{\text{proj}} = (I + \mu P)^{-1} \Delta W_c. \quad (24)$$

b) Simplifying the inverse.: Since $P = V_k V_k^\top$ is a rank- k projector with $V_k^\top V_k = I_k$, the inverse matrix admits the closed form

$$(I + \mu P)^{-1} = I - \frac{\mu}{1+\mu} V_k V_k^\top, \quad (25)$$

which follows from either spectral decomposition or the Woodbury identity.

Substituting (25) into (24), we obtain the soft projection operator

$$P_{\text{soft}} = I - \frac{\mu}{1+\mu} V_k V_k^\top, \quad \Delta W_c^{\text{proj}} = P_{\text{soft}} \Delta W_c. \quad (26)$$

c) Final fusion rule.: The merged LoRA is then defined as

$$\Delta W_m = \Delta W_s + \Delta W_c^{\text{proj}} = \Delta W_s + \left(I - \frac{\mu}{1+\mu} V_k V_k^\top\right) \Delta W_c. \quad (27)$$

This formulation continuously interpolates between direct merging ($\mu = 0$) and hard projection ($\mu \rightarrow \infty$), offering a controllable balance between style preservation and content retention.

VIII. RANDOMLY SAMPLING LORA PAIRS.

Following prior works including K-LoRA [8] (18 pairs) and ZipLoRA [7] (32 pairs), we evaluate our NP-LoRA on **32 randomly sampled content–style LoRA pairs**, covering **5 animal subjects**, **5 object-level categories**, and **15 distinct artistic styles**.

The specific content–style combinations are listed below:

dog	in watercolor painting style3, in kid crayon drawing style, in oil painting style3, in watercolor painting style2
cat2	in watercolor painting style3, in oil painting style1, in oil painting style2
dog2	in sticker style, in watercolor painting style3, in oil painting style3
vase	in line drawing style, in oil painting style3, in sticker style
candle	in 3d rendering style2, in kid crayon drawing style, in watercolor painting style2
colorful_sneaker	in watercolor painting style1, in line drawing style, in wooden sculpture
bear_plushie	in oil painting style2, in wooden sculpture, in 3d rendering style
dog5	in cartoon line drawing style, in glowing 3d rendering style
wolf_plushie	in flat cartoon illustration style, in abstract rainbow colored flowing smoke wave design, in 3d rendering style
dog8	in cartoon line drawing style, in flat cartoon illustration style, in glowing 3d rendering style, in sticker style

The naming of content categories and artistic styles strictly follows the conventions used in publicly released codebases, consistent with K-LoRA [6], [47]. Readers may refer to the corresponding open-source implementations for qualitative visualizations of each content–style pair.

IX. IMPLEMENTATION DETAILS

In our theoretical formulation, we employ the singular value decomposition (SVD) to obtain the right singular subspace of

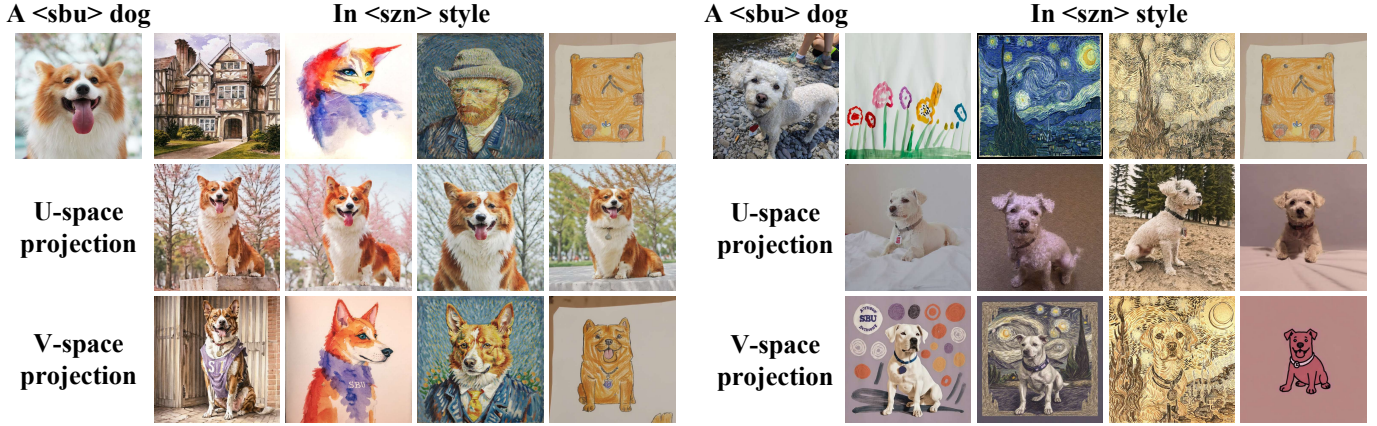


Fig. 8. Comparison of output-space (U) and parameter-space (V) projections for null-space construction. The U-space projection fails to remove style interference, leading to distorted stylistic features, whereas the V-space projection effectively eliminates such interference and preserves the intended style appearance.

the LoRA update matrix $\Delta W_s = B_s A_s$, where $A_s \in \mathbb{R}^{r \times n}$ and $B_s \in \mathbb{R}^{m \times r}$. Specifically, the original projection of ΔW_c onto the orthogonal complement of ΔW_s is computed using the right singular vectors V_k of ΔW_s , i.e.,

$$\Delta W_c^\perp = \Delta W_c (I - V_k V_k^\top). \quad (28)$$

However, directly computing V_k via SVD or PCA on the large matrix $\Delta W_s \in \mathbb{R}^{m \times n}$ is computationally expensive, as its complexity scales with $\mathcal{O}(mnr)$.

a) *Efficient QR-based implementation.*: To improve efficiency, we replace the SVD with a QR-based projection that is mathematically equivalent but far more efficient. Observe that ΔW_s has rank at most r and its right singular subspace is equal to the column space of A_s^\top :

$$\text{span}(V) = \text{span}(A_s^\top). \quad (29)$$

Therefore, we compute a thin QR decomposition on A_s^\top :

$$A_s^\top = QR, \quad (30)$$

where $Q \in \mathbb{R}^{n \times r}$ has orthonormal columns spanning $\text{span}(A_s^\top)$, and $R \in \mathbb{R}^{r \times r}$ is an upper triangular matrix. We then replace V with Q and compute

$$\Delta W_c^{\text{proj}} = \Delta W_c - \Delta W_c Q Q^\top, \quad (31)$$

which requires only a QR decomposition of a small matrix of size $n \times r$ (where $r \ll n, m$), reducing complexity to $\mathcal{O}(nr^2)$.

b) *Proof of equivalence.*: Let $\Delta W_s = B_s A_s$ denote the LoRA matrix. Since LoRA uses low-rank factors ($A_s \in \mathbb{R}^{r \times n}$) and ($B_s \in \mathbb{R}^{m \times r}$) with full column and row rank (i.e., $\text{rank} = r$), $(B_s^\top B_s)$ is symmetric positive definite. Then

$$\Delta W_s^\top \Delta W_s = A_s^\top (B_s^\top B_s) A_s. \quad (32)$$

Since $B_s^\top B_s$ is symmetric positive definite, it admits a Cholesky factorization $B_s^\top B_s = C^\top C$ with C invertible. Substituting gives

$$\Delta W_s^\top \Delta W_s = (C A_s)^\top (C A_s). \quad (33)$$

As C represents a full-rank linear transform, it does not alter the column space of A_s^\top . Hence, the right singular subspace

of ΔW_s coincides with $\text{span}(A_s^\top)$:

$$\text{Col}(\Delta W_s^\top \Delta W_s) = \text{span}(A_s^\top). \quad (34)$$

Therefore, the orthogonal projectors constructed via SVD and QR are identical:

$$P = V_k V_k^\top = Q Q^\top. \quad (35)$$

In practice, this means that replacing the expensive low-rank SVD with a simple QR decomposition of A_s^\top yields a mathematically equivalent projection while reducing computation time by an order of magnitude.

X. WHICH NULL-SPACE CONSTRUCTION PRESERVES STYLE: U-SPACE OR V-SPACE?

In the main paper, we construct the null space using the right singular vectors V from the SVD decomposition $\Delta W_s = U \Sigma V^\top$, since interference in LoRA fusion occurs in the parameter space (i.e., the column space of ΔW_s) rather than in the activation space represented by U . Specifically, U spans the output (activation) domain of ΔW_s , describing how style LoRA influences feature activations, while V spans the input (parameter) domain, capturing how LoRA updates are distributed across the weight columns. Because LoRA fusion directly manipulates weight parameters, interference emerges along these column directions, making V the appropriate basis for constructing the null space. Projecting in the V -space thus directly eliminates content-induced perturbations along the style-critical directions within the weight domain. In contrast, constructing the null space based on U operates in the output (activation) space, which suppresses both content and style responses and weakens overall expressiveness. As shown in Fig. 8, projections built from V effectively preserve stylistic consistency, while those derived from U fail to disentangle content and style, resulting in noticeable style degradation.

XI. ADDITIONAL ABLATION ON SOFT PROJECTION

We refer to the version without soft relaxation as the hard variant, denoted as NP-LoRA-H. The qualitative results are

TABLE IV
COMPARISON WITH JOINT TRAINING METHOD USING CLIP AND DINO
SIMILARITY SCORES FOR CONTENT PRESERVATION AND STYLE
ALIGNMENT. ONLY THE AGGREGATED RESULTS (S_{ARITH} AND S_{HARM})
REFLECT THE OVERALL TRADE-OFF BETWEEN CONTENT AND STYLE;
THUS, ONLY THESE TWO COLUMNS ARE EMPHASIZED.

Method	$S_{\text{content}}^{\text{CLIP}}$	$S_{\text{style}}^{\text{CLIP}}$	$S_{\text{content}}^{\text{DINO}}$	$S_{\text{style}}^{\text{DINO}}$	S_{arith}	$S_{\text{harm}} \uparrow$
Joint Training	0.67	0.61	0.49	0.25	0.50	0.43
NP-LoRA-H	0.68	0.60	0.39	0.40	0.52	0.48
NP-LoRA	0.73	0.59	0.52	0.33	0.55	0.50

shown in Fig. 9, and the quantitative comparison is provided in Tab. IV. As illustrated, NP-LoRA-H effectively preserves the style but tends to lose content details. In contrast, our full NP-LoRA achieves a better balance between content and style, yielding the highest overall scores. This confirms the necessity of the proposed soft relaxation mechanism.

XII. ADDITIONAL COMPARISON WITH JOINT TRAINING

We further compare our method with joint training baseline, where a new LoRA is trained from scratch using mixed content and style images. The qualitative results are shown in Fig. 9, and the quantitative comparison is provided in Tab. IV. As observed, the joint-training approach exhibits high instability, i.e., while it occasionally produces reasonable fusion, it often fails to effectively combine content and style. This instability may arise from catastrophic forgetting during multi-objective optimization, where learning new style features interferes with previously acquired content representations. In contrast, our NP-LoRA achieves consistent and harmonious fusion without any retraining, effectively preserving both content fidelity and stylistic characteristics. Quantitatively, as shown in Table IV, NP-LoRA outperforms joint training across all metrics, with NP-LoRA achieving the highest overall score, confirming its superior ability to preserve content and style simultaneously.

XIII. PROMPT CONTROL

We conduct experiments to assess whether our method can alter the object’s actions, the surrounding environment, or introduce new elements by adjusting the prompts. As shown in 10, after modifying the prompts, our method effectively preserves the original object’s characteristics and stylistic attributes, while seamlessly integrating new elements or scene details.

XIV. ROBUSTNESS TEST

We evaluate the robustness of our method by running experiments with different random seeds to examine stability across stochastic conditions. As shown in Fig. 11, our approach produces consistently stable results under varying seeds, matching the qualitative trends observed in the main paper. Specifically, NP-LoRA achieves a balanced trade-off between content preservation and style consistency, yielding the most visually harmonious results.

XV. FURTHER GENERALIZATION VALIDATION ON FLUX

To further validate the generality of NP-LoRA, we apply our method to the FLUX backbone using publicly available LoRAs covering diverse subjects and styles. As shown in Fig. 12, 13, NP-LoRA consistently preserves the balance between subject identity and stylistic fidelity across various domains. These results demonstrate that our projection-based fusion mechanism remains effective even under different diffusion architectures, highlighting the robustness and general applicability of the proposed approach.

a) Prompt used for GPT-5 evaluation.:

Task: Evaluate and select the candidate image that best balances Subject Fidelity and Style Consistency.
Inputs: - First image = A.jpg (Subject Fidelity reference): core subject content to preserve. - Second image = B.jpg (Style reference): artistic style, colors, lighting to apply. - Next six images are candidates, named [Model_1]..[Model_6] in the given order.
Candidate mapping (fixed): [Model_1] = Direct [Model_2] = Klora [Model_3] = LoRARar [Model_4] = B-LoRA [Model_5] = ziplora [Model_6] = NP-LoRA
Evaluation Criteria: 1) Subject Fidelity: retain key characteristics/structure/recognizability from A.jpg. 2) Style Consistency: apply style/texture/colors/lighting present in B.jpg.
Crucial Requirement: Do not choose images that only retain the subject without the style, or only mimic the style with distorted subject. Select the BEST BALANCE.
Output Rules (IMPORTANT): You MUST respond with ONLY ONE of the following exact strings (case-sensitive): Direct Klora LoRARar B-LoRA ziplora NP-LoRA Do NOT output anything else. Do NOT include punctuation, brackets, markdown, or explanation.

XVI. DETAILS FOR GPT-5 EVALUATION PROTOCOL

In the main paper, we employed the GPT-5 model to automatically evaluate and select the candidate image that best balances Subject Fidelity and Style Consistency. The exact prompt used for GPT-5 is listed below to ensure full reproducibility.

During evaluation, GPT-5 received the reference subject image (A. jpg), the reference style image (B. jpg), and six generated candidates from different merging strategies. It then followed the above prompt to independently select the best-balanced image. Each case was judged in isolation to prevent cross-sample bias. The final GPT-5 preference score reported represents the proportion of cases where each method was selected as the best overall result.

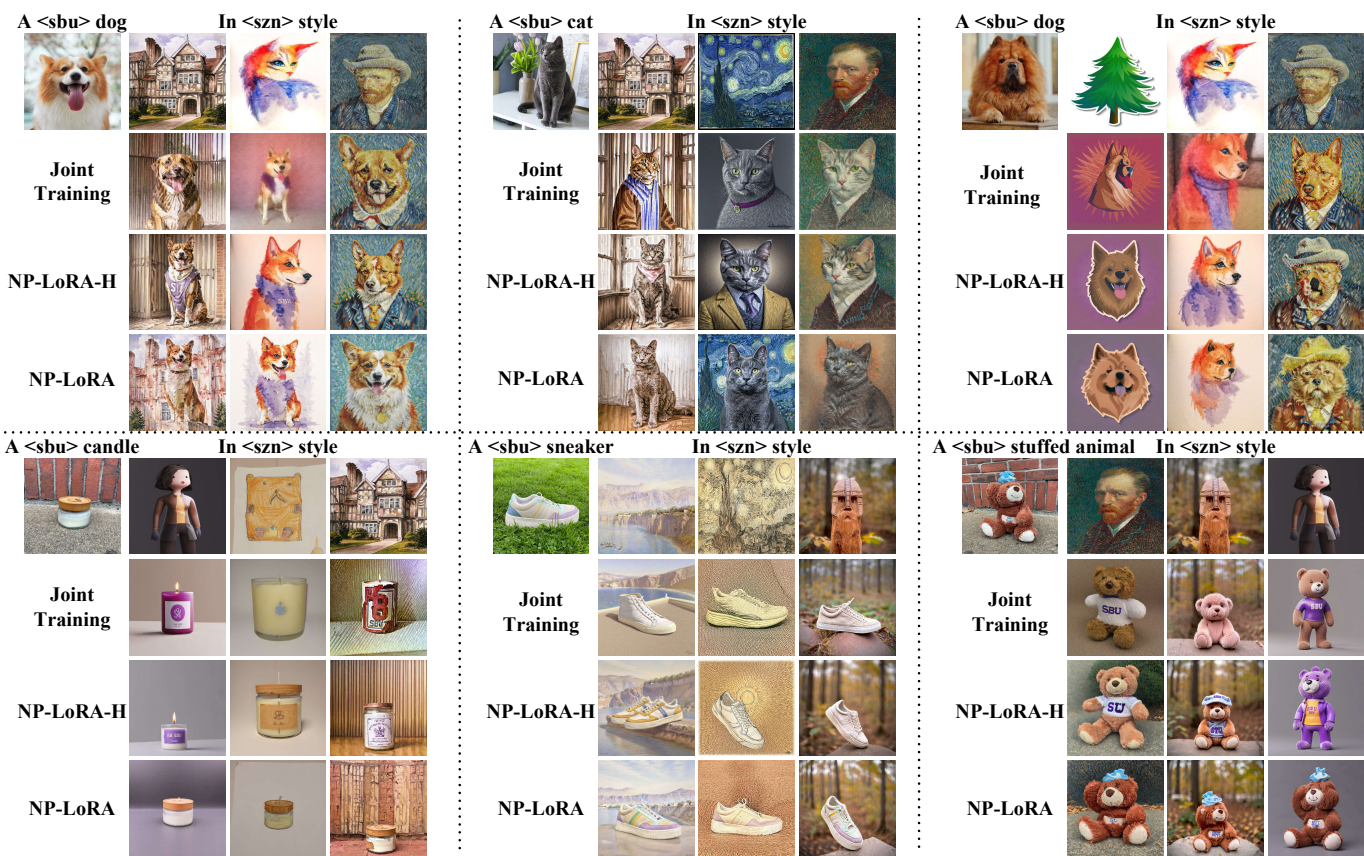


Fig. 9. Qualitative comparison with joint training. Joint training exhibits unstable performance and often fails to merge content and style effectively, while N-LoRA achieves consistent and well-balanced fusion without retraining.

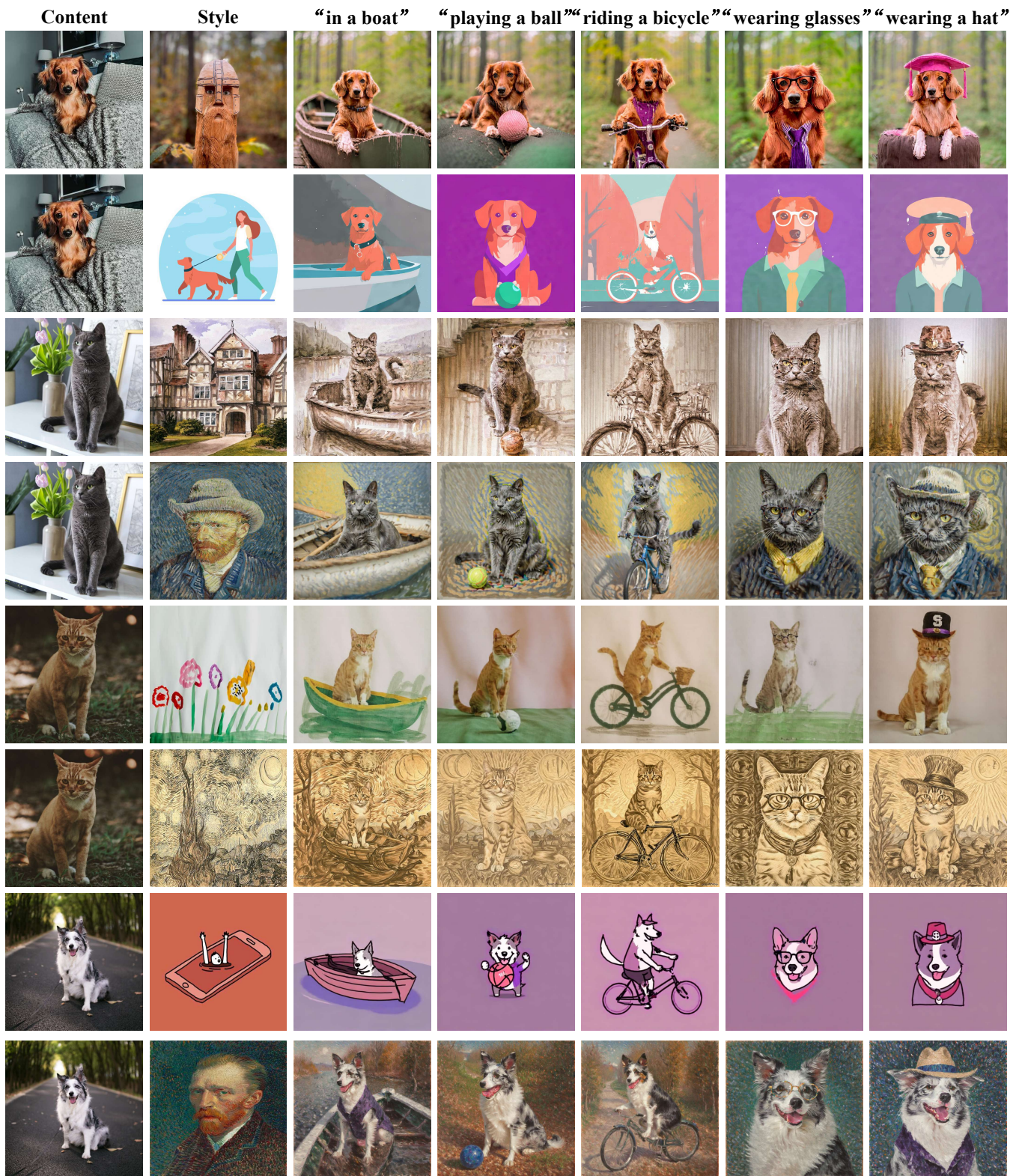


Fig. 10. Our method effectively modifies the object’s actions and environment while maintaining the original style.

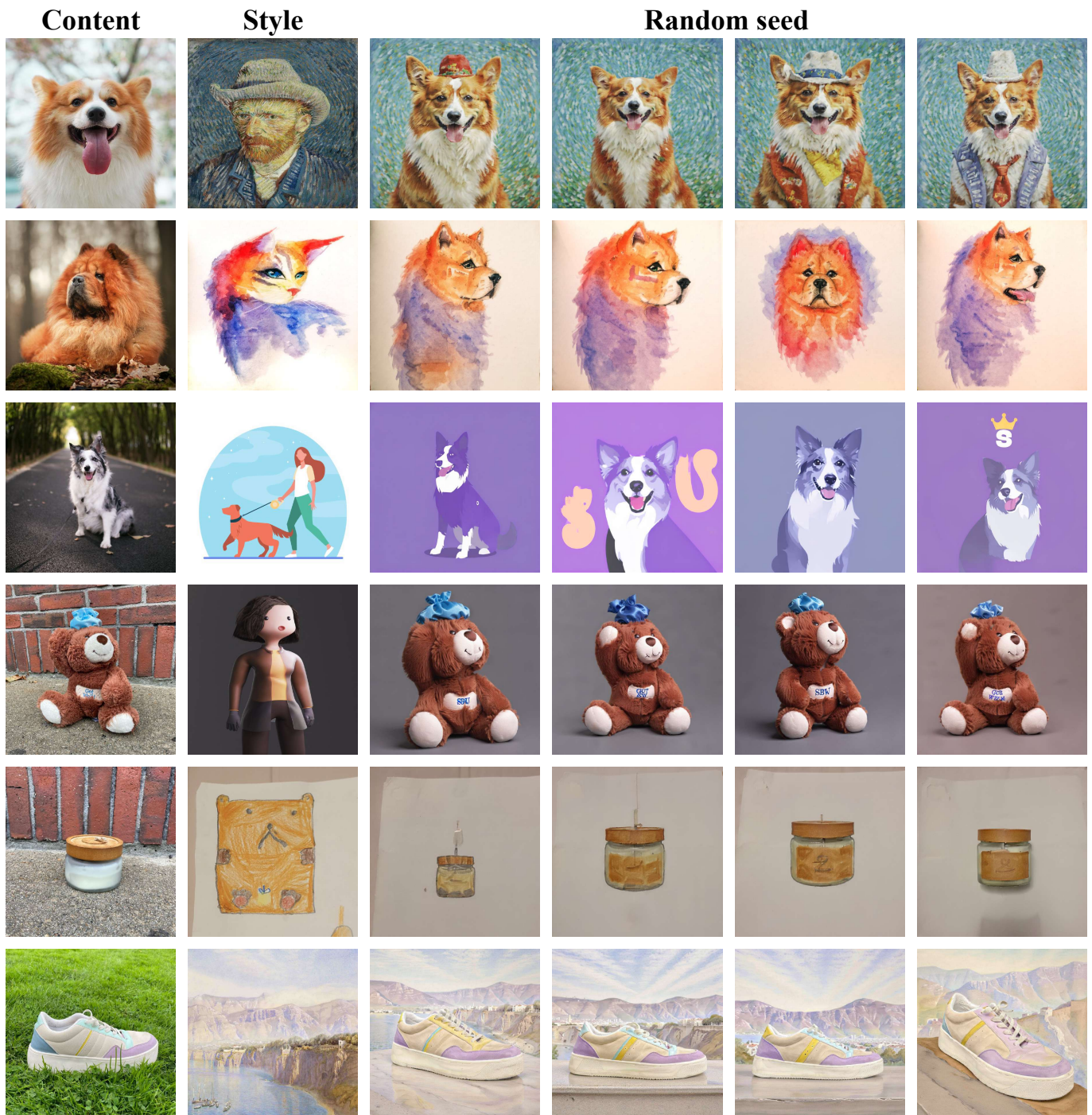


Fig. 11. Results obtained with randomly selected seeds demonstrate the stability and robustness of our NP-LoRA.

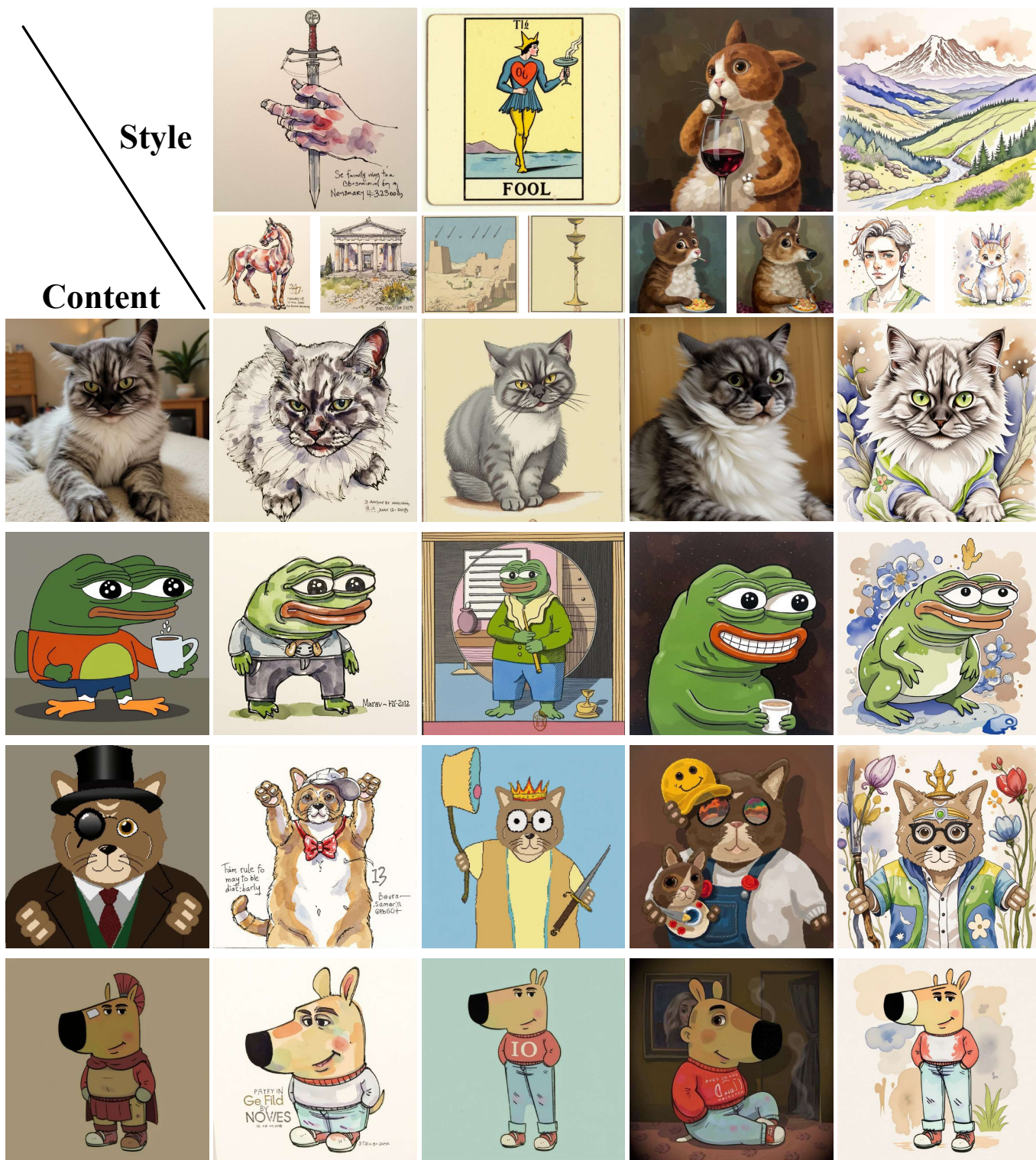


Fig. 12. Qualitative results of NP-LoRA on the Flux backbone using diverse publicly available LoRAs. Each image corresponds to the combination of the content LoRA shown above and the style LoRA shown on the left, illustrating the results produced by our method.

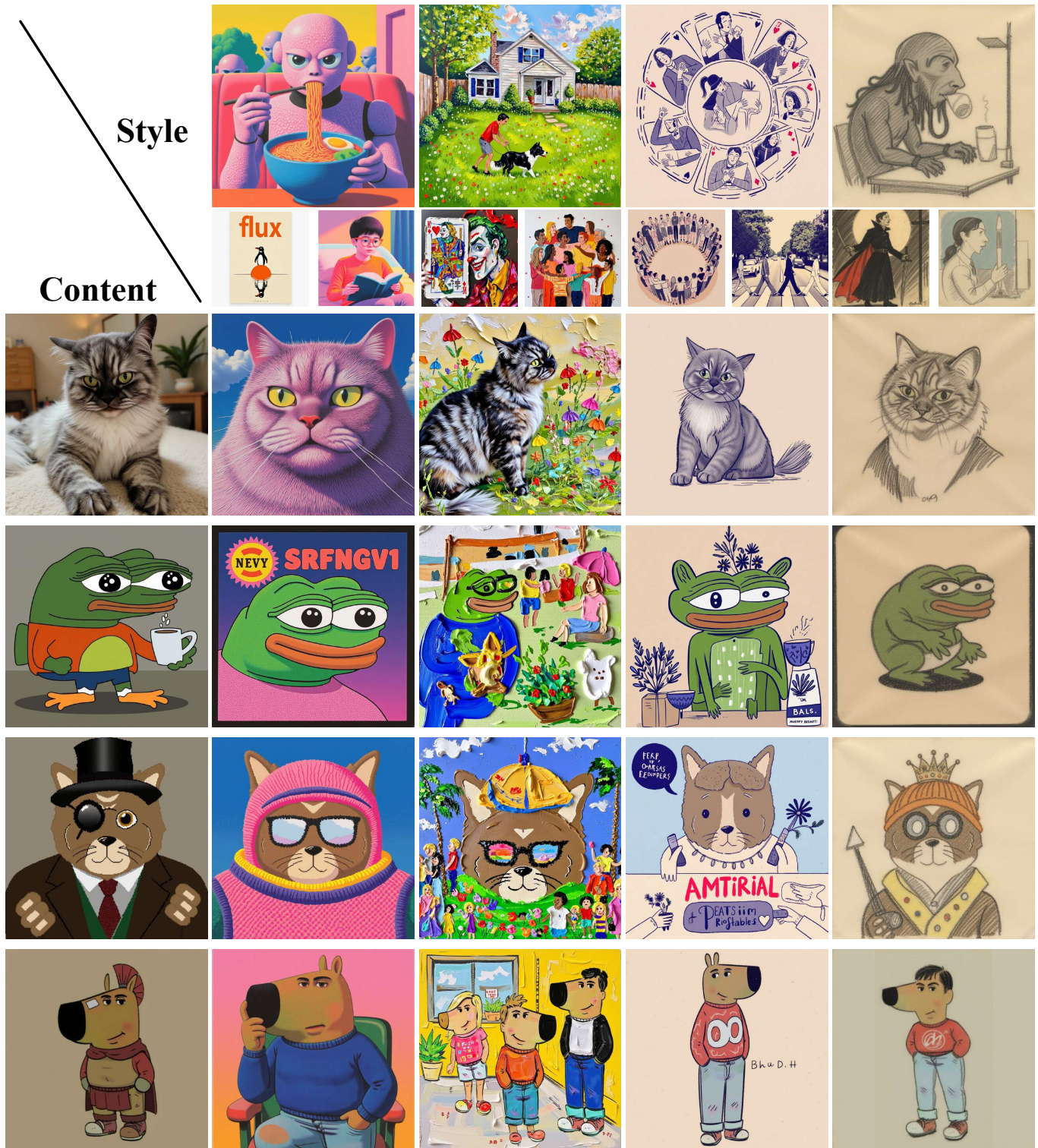


Fig. 13. Qualitative results of NP-LoRA on the Flux backbone using diverse publicly available LoRAs. Each image corresponds to the combination of the content LoRA shown above and the style LoRA shown on the left, illustrating the results produced by our method.